

Long-Range triplet Josephson Current Modulated by the Interface Magnetization Texture

Hao Meng, Xiuqiang Wu, and Zhiming Zheng

National Laboratory of Solid State Microstructures and Department of Physics, Nanjing University, Nanjing 210093, China
(Dated: July 27, 2018)

We have investigated the Josephson coupling between two s-wave superconductors separated by the ferromagnetic trilayers with noncollinear magnetization. We find that the long-range triplet critical current will oscillate with the strength of the exchange field and the thickness of the interface layer, when the interface magnetizations are orthogonal to the central magnetization. This feature is induced by the spatial oscillations of the spin-triplet state $|\uparrow\downarrow\rangle+|\downarrow\uparrow\rangle$ in the interface layer. Moreover, the critical current can exhibit a characteristic nonmonotonic behavior, when the misalignment angle between interface magnetization and central ferromagnet increases from 0 to $\pi/2$. This peculiar behavior will take place under the condition that the original state of the junction with the parallel magnetizations is the π state.

PACS numbers: 74.78.Fk, 73.40.-c, 74.50.+r, 73.63.-b

I. INTRODUCTION

The interplay between ferromagnetism and superconductivity in hybrid structures has recently attracted considerable attention because of the underlying rich physics and potential applications in spintronics^{1,2}. In a homogeneous ferromagnet (F) adjacent to an s-wave superconductor (S), the Cooper pairs, in which two electrons have opposite spins and momenta ($\mathbf{k}\uparrow, -\mathbf{k}\downarrow$), can penetrate into the F a short-range. In this case, superconducting correlations between pairs of electrons are induced in both the spin-singlet component $|\uparrow\downarrow\rangle-|\downarrow\uparrow\rangle$ (afterwards, the normalizing factor $1/\sqrt{2}$ is omitted for brevity) and the spin-triplet component $|\uparrow\downarrow\rangle+|\downarrow\uparrow\rangle$ with zero spin projection along the magnetization axis. Accordingly, an opposite-spin Cooper pair $|\uparrow\downarrow\rangle$ acquires the total momentum Q or $-Q$ inside the ferromagnet as a response to the exchange splitting $2h_0$ between the spin up and spin down bands³. Here $Q \simeq 2h_0/\hbar v_F$, where v_F is the Fermi velocity. The resulting state is a mixture of singlet component and triplet component with zero total spin projection: $(|\uparrow\downarrow\rangle-|\downarrow\uparrow\rangle)\cos(Q\cdot R)+i\cdot(|\uparrow\downarrow\rangle+|\downarrow\uparrow\rangle)\sin(Q\cdot R)$. These two components oscillate in F with the same period but their phases differ by $\pi/2$.

In contrast, more interesting the long-range triplet component with parallel electron spins can be induced by the noncollinear magnetic configuration⁴⁻⁶. This component penetrates into the ferromagnet over a large distance, which can be on the order of the normal metal coherence length ξ_N in some cases. The reason is that the component with parallel spins is not as sensitive to the exchange field as the opposite-spin component. In order to observe this effect, Houzet *et al.*⁷ suggests measuring the critical current in a Josephson junction through a ferromagnetic trilayers with noncollinear magnetizations. In this geometry, the interface magnetization is in a different direction with the central F layer. This noncollinear magnetic configuration leads to spin-flip scattering processes at the interfaces. It can convert the triplet pairs $|\uparrow\downarrow\rangle+|\downarrow\uparrow\rangle$ into the equal-spin pairs $|\uparrow\uparrow\rangle$ or $|\downarrow\downarrow\rangle$, and

that equal-spin pairs may propagate coherently over long distances into the central F layer. A maximal critical current is obtained when the interface layers have a thickness comparable to the ferromagnetic coherence length ξ_F , and the magnetizations in successive layers are orthogonal. Moreover, Alidoust *et al.*⁸ replace the interface homogeneous F layers with the spiral ferromagnetic layers and domainwall ferromagnets. They find a synthesis of $0-\pi$ oscillations with superimposed rapid oscillations when varying the width of the interface layer. Indeed, many recent experiments have measured a strong enhancement of the long-range Josephson current through a ferromagnetic multilayer with noncollinear magnetizations⁹⁻¹¹. Theoretically, Hikino *et al.*¹² shows that the long-range spin current can be driven by the superconducting phase difference in a Josephson junction with double layer ferromagnets. Such spin current carried by the spin-triple Cooper pairs exhibits long-range propagation in the F even when the Josephson charge current is practically zeros.

In this paper, we adopt Blonder, Tinkham, and Klapwijk (BTK) approach¹³ and Bogoliubov's self-consistent field method¹⁴ to study the critical Josephson current in clean S/ F_1 / F_2 / F_3 /S junction with noncollinear magnetization. We propose that the long-range triplet critical current can be modulated by varying the strength of exchange field and thickness of interface ferromagnet, when the interface magnetizations are orthogonal to the central magnetization. This feature is induced by the spatial oscillation of the triplet state $|\uparrow\downarrow\rangle+|\downarrow\uparrow\rangle$ in the interface region. In addition, the critical current manifests a characteristic nonmonotonic behavior, when the misalignment angle between interface magnetization and central ferromagnet changes from 0 to $\pi/2$. This peculiar behavior will appear when the π state is the original state of the junction on condition that the ferromagnetic trilayers have the parallel magnetizations.

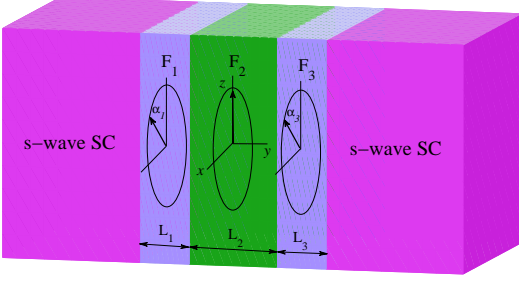


FIG. 1. (color online) Schematic illustration of the S/F₁/F₂/F₃/S junction. The magnetization vectors lie in the x - z plane and three arrows indicate the direction of magnetizations in F_1 , F_2 and F_3 . The phase difference between the two s-wave Ss is $\varphi = \phi_R - \phi_L$.

II. MODEL AND FORMULA

We study a clean Josephson junction formed of two s-wave Ss contacted through three F layers with non-collinear magnetization (see fig. 1). For convenience, we denote the three ferromagnetic layers sequentially by F_1 , F_2 and F_3 . The three F layers have the thickness L_1 , L_2 , L_3 , and the exchange field h_1 , h_2 , h_3 . The transport direction is along the y axis, and the system is assumed to be infinite in the x - z plane.

The BCS mean-field effective Hamiltonian^{1,14} is

$$H_{eff} = \int d\vec{r} \left\{ \sum_{\tilde{\alpha}} \psi_{\tilde{\alpha}}^{\dagger}(\vec{r}) H_e \psi_{\tilde{\alpha}}(\vec{r}) + \frac{1}{2} \left[\sum_{\tilde{\alpha}, \tilde{\beta}} (i\sigma_y)_{\tilde{\alpha}\tilde{\beta}} \Delta(\vec{r}) \psi_{\tilde{\alpha}}^{\dagger}(\vec{r}) \psi_{\tilde{\beta}}^{\dagger}(\vec{r}) + H.C. \right] - \sum_{\tilde{\alpha}, \tilde{\beta}} \psi_{\tilde{\alpha}}^{\dagger}(\vec{r}) (\vec{h} \cdot \vec{\sigma})_{\tilde{\alpha}\tilde{\beta}} \psi_{\tilde{\beta}}(\vec{r}) \right\}, \quad (1)$$

where $H_e = -\nabla^2/2m - E_F$, $\psi_{\tilde{\alpha}}^{\dagger}(\vec{r})$ and $\psi_{\tilde{\alpha}}(\vec{r})$ are creation and annihilation operators with spin $\tilde{\alpha}$. $\vec{\sigma}$ is the Pauli matrices, m is the effective mass of the quasiparticles in both Ss and Fs, and E_F is the Fermi energy. The superconducting gap is denoted by $\Delta(\vec{r}) = \Delta(T)[e^{i\phi_L}\Theta(-y) + e^{i\phi_R}\Theta(y - L_F)]$ with $L_F = L_1 + L_2 + L_3$. Here, $\Delta(T)$ accounts for the temperature-dependent energy gap that satisfies the BCS relation $\Delta(T) = \Delta_0 \tanh(1.74\sqrt{T_c/T - 1})$ with T_c the critical temperature of the Ss. $\phi_{L(R)}$ is the phase of the left (right) S and $\Theta(y)$ is the unit step function. The exchange field \vec{h} due to the ferromagnetic magnetizations in the F_i ($i=1, 2, 3$) layers is described by $\vec{h} = h_i(\sin\alpha_i\hat{e}_x + \cos\alpha_i\hat{e}_z)$, where α_i is the polar angle of the magnetization, and $\hat{e}_{x(z)}$ is the unit vector along the $x(z)$ direction.

By using the Bogoliubov transformation $\psi_{\tilde{\alpha}}(\vec{r}) = \sum_n [u_{n\tilde{\alpha}}(\vec{r})\hat{\gamma}_n + v_{n\tilde{\alpha}}^*(\vec{r})\hat{\gamma}_n^{\dagger}]$ and the anticommutation relations of the quasiparticle annihilation and creation operators $\hat{\gamma}_n$ and $\hat{\gamma}_n^{\dagger}$, we have the Bogoliubov-de Gennes

(BdG) equation^{1,14},

$$\check{H}\Psi(\vec{r}) = E\Psi(\vec{r}), \quad (2)$$

where

$$\check{H} = \begin{pmatrix} \hat{H}(\vec{r}) & \hat{\Delta}(\vec{r}) \\ -\hat{\Delta}^*(\vec{r}) & -\hat{H}(\vec{r}) \end{pmatrix},$$

$\hat{H}(\vec{r}) = H_e \hat{\mathbf{1}} - h_z(\vec{r})\hat{\sigma}_z - h_x(\vec{r})\hat{\sigma}_x$ and $\hat{\Delta}(\vec{r}) = i\Delta(\vec{r})\hat{\sigma}_y$. Here, $\hat{\mathbf{1}}$ is the unity matrix, $\Psi(\vec{r}) = (u_{\uparrow}(\vec{r}), u_{\downarrow}(\vec{r}), v_{\uparrow}(\vec{r}), v_{\downarrow}(\vec{r}))^T$ is four-component wave function. The BdG equation can be solved for each superconductor lead and each ferromagnetic layer, respectively. We can have four different incoming quasiparticles, electronlike quasiparticles (ELQs) and holelike quasiparticles (HLQs) with spin up and spin down. For an incident spin-up electron in the left superconductor, the wave function is

$$\begin{aligned} \Psi_L^S(y) = & [ue^{i\phi_L/2}, 0, 0, ve^{-i\phi_L/2}]^T e^{ik_e y} \\ & + a_1 [ve^{i\phi_L/2}, 0, 0, ue^{-i\phi_L/2}]^T e^{ik_h y} \\ & + b_1 [ue^{i\phi_L/2}, 0, 0, ve^{-i\phi_L/2}]^T e^{-ik_e y} \\ & + a'_1 [0, -ve^{i\phi_L/2}, ue^{-i\phi_L/2}, 0]^T e^{ik_h y} \\ & + b'_1 [0, ue^{i\phi_L/2}, -ve^{-i\phi_L/2}, 0]^T e^{-ik_e y}. \end{aligned} \quad (3)$$

In this process, the coefficients b_1 , b'_1 , a'_1 , and a_1 describe normal reflection, the normal reflection with spin-flip, novel Andreev reflection, and usual Andreev reflection, respectively. We note that the momentum parallel to the interface is conserved for these processes.

The corresponding wave function in the right superconductor is

$$\begin{aligned} \Psi_R^S(y) = & c_1 [ue^{i\phi_R/2}, 0, 0, ve^{-i\phi_R/2}]^T e^{ik_e y} \\ & + d_1 [ve^{i\phi_R/2}, 0, 0, ue^{-i\phi_R/2}]^T e^{-ik_h y} \\ & + c'_1 [0, ue^{i\phi_R/2}, -ve^{-i\phi_R/2}, 0]^T e^{ik_e y} \\ & + d'_1 [0, -ve^{i\phi_R/2}, ue^{-i\phi_R/2}, 0]^T e^{-ik_h y}, \end{aligned} \quad (4)$$

where c_1 , d_1 , c'_1 , d'_1 are the transmission coefficients, corresponding to the reflection processes described above. The coherence factors are defined as usual, $u = \sqrt{(1 + \Omega/E)/2}$, $v = \sqrt{(1 - \Omega/E)/2}$ and $\Omega = \sqrt{E^2 - \Delta^2}$. $k_{e(h)} = \sqrt{2m[E_F + (-)\Omega]/\hbar^2 - k_{\parallel}^2}$ are the perpendicular components of the wavevectors with k_{\parallel} as the parallel component.

The wave function in the F_i layers can be described by transformation matrix¹⁵ as

$$\begin{aligned} \Psi_i^F(y) = & T_i \{ [e \cdot \exp(ik_{F_i}^{\uparrow} y) + f \cdot \exp(-ik_{F_i}^{\uparrow} y)] \hat{e}_1 \\ & + [e' \cdot \exp(ik_{F_i}^{\downarrow} y) + f' \cdot \exp(-ik_{F_i}^{\downarrow} y)] \hat{e}_2 \\ & + [g \cdot \exp(-ik_{F_i}^{\uparrow} y) + h \cdot \exp(ik_{F_i}^{\uparrow} y)] \hat{e}_3 \\ & + [g' \cdot \exp(-ik_{F_i}^{\downarrow} y) + h' \cdot \exp(ik_{F_i}^{\downarrow} y)] \hat{e}_4 \}. \end{aligned} \quad (5)$$

Here $\hat{e}_1 = [1, 0, 0, 0]^T$, $\hat{e}_2 = [0, 1, 0, 0]^T$, $\hat{e}_3 = [0, 0, 1, 0]^T$, $\hat{e}_4 = [0, 0, 0, 1]^T$ are basis wave functions, and $k_{F_i}^{e(h)\sigma} =$

$\sqrt{2m[E_F + (-)E + \rho_\sigma h_i]/\hbar^2 - k_\parallel^2}$ with $\rho_{\uparrow(\downarrow)}=1(-1)$ are the perpendicular components of wave vectors for ELQs and HLQs. The transformation matrix is defined as $T_i = \hat{\mathbf{1}} \otimes (\cos \frac{\alpha_i}{2} \cdot \hat{\mathbf{1}} - i \cdot \sin \frac{\alpha_i}{2} \cdot \hat{\sigma}_y)$. All scattering coefficients can be determined by solving wave functions at the interfaces.

$$\Psi_L^S(0) = \Psi_1^F(0), \partial_y[\psi_1^F - \psi_L^S]|_{y=0} = 2k_F Z_1 \psi_1^F(0); \quad (6)$$

$$\begin{aligned} \Psi_{i-1}^F(y_{i-1}) &= \Psi_i^F(y_{i-1}), \\ \partial_y[\psi_i^F - \psi_{i-1}^F]|_{y=y_{i-1}} &= 2k_F Z_i \psi_i^F(y_{i-1}); \end{aligned} \quad (7)$$

$$\Psi_R^S(L_F) = \Psi_3^F(L_F), \partial_y[\psi_R^S - \psi_3^F]|_{y=L_F} = 2k_F Z_4 \psi_R^S(L_F). \quad (8)$$

Where $Z_1 \sim Z_4$ are dimensionless parameters describing the magnitude of the interfacial resistances. y_i is local coordinate value at the F_i/F_{i+1} interface, and $k_F = \sqrt{2mE_F}$ is the Fermi wave vector. From the boundary conditions, we obtain a system of linear equations that yield the scattering coefficients. With the scattering coefficients at hand, we can use the finite-temperature Green's function formalism¹⁶⁻¹⁸ to calculate dc Josephson current,

$$\begin{aligned} I_e(\varphi) &= \frac{k_B T e \Delta}{4\hbar} \sum_{k_\parallel} \sum_{\omega_n} \frac{k_e(\omega_n) + k_h(\omega_n)}{\Omega_n} \\ & \left[\frac{a_1(\omega_n, \varphi) - a_2(\omega_n, \varphi)}{k_e} + \frac{a_3(\omega_n, \varphi) - a_4(\omega_n, \varphi)}{k_h} \right], \end{aligned} \quad (9)$$

where $\omega_n = \pi k_B T (2n + 1)$ is the Matsubara frequencies with $n=0, 1, 2, \dots$ and $\Omega_n = \sqrt{\omega_n^2 + \Delta^2(T)}$. $k_e(\omega_n)$, $k_h(\omega_n)$, and $a_j(\omega_n, \varphi)$ with $j=1, 2, 3, 4$ are obtained from k_e , k_h , and a_j by analytic continuation $E \rightarrow i\omega_n$. We find the critical current from $I_c = \text{Max}_\varphi |I_e(\varphi)|$.

The above results for Josephson current in the clean limit are obtained in the stepwise approximation for the pair potential. To obtain the time dependent triplet amplitude functions and the local density of the states (LDOS), we solve the BdG equation (2) by Bogoliubov's self-consistent field method^{14,19-21}. We put the junction in a one dimensional square potential well with infinitely high walls. Accordingly, the solution in equation (2) can be expanded a set of basis vectors of the stationary states²², $u_\sigma(\vec{r}) = \sum_q u_q^\sigma \zeta_q(y)$ and $v_\sigma(\vec{r}) = \sum_q v_q^\sigma \zeta_q(y)$ with $\zeta_q(y) = \sqrt{2/L_d} \sin(q\pi y/L_d)$. Here q is a positive integer, and $L_d = L_{S1} + L_F + L_{S2}$, L_{S1} and L_{S2} are thickness of left and right superconductors, respectively. The BdG equation (2) is solved iteratively together with the self-consistency condition¹⁴

$$\Delta(y) = \frac{g(y)}{2} \sum_{0 \leq E \leq \omega_D} [u_\uparrow(y)v_\downarrow^*(y) - u_\downarrow(y)v_\uparrow^*(y)] \tanh\left(\frac{E}{2k_B T}\right), \quad (10)$$

where ω_D is the Debye cutoff energy and the effective attractive coupling $g(y)$ is a constant in the superconductor and can vanish outside of it. Iterations are not

performed until self-consistency is reached, starting from the stepwise approximation for the pair potential. The amplitudes of the triplet pair are defined as follows^{20,21}

$$f_0(y, t) = \frac{1}{2} \sum_{E>0} [u_\uparrow(y)v_\downarrow^*(y) + u_\downarrow(y)v_\uparrow^*(y)] S(t), \quad (11)$$

$$f_1(y, t) = \frac{1}{2} \sum_{E>0} [u_\uparrow(y)v_\uparrow^*(y) - u_\downarrow(y)v_\downarrow^*(y)] S(t), \quad (12)$$

where $S(t) = \cos(Et) - i \sin(Et) \tanh(E/2k_B T)$. Additionally, the singlet pair amplitude writes as $f_3 \equiv \Delta(y)/g(y)$. The above singlet and triplet pair amplitudes are all normalized to the value of the singlet pairing amplitude in a bulk S material. The LDOS is given by

$$N(y, \varepsilon) = - \sum_{\tilde{\alpha}} [u_{\tilde{\alpha}}^2(y) f'(\varepsilon - E) + v_{\tilde{\alpha}}^2(y) f'(\varepsilon + E)], \quad (13)$$

where $f'(\varepsilon) = \partial f / \partial \varepsilon$ is the derivative of the Fermi function. The LDOS is normalized by its value at $\varepsilon = 3\Delta_0$ beyond which the LDOS is almost constant.

III. RESULTS AND DISCUSSIONS

In BTK approach, we will use the superconducting gap Δ_0 as the unit of energy. The Fermi energy is $E_F = 1000\Delta_0$, the interface transparency is $Z_{1-4} = 0$, and $T/T_c = 0.1$. We fix the thickness of the F_2 layer $k_F L_2 = 200$, the exchange field $h_2/E_F = 0.6$, and the magnetization direction along the z direction that equivalents to $\alpha_2 = 0$. Interface layers F_1 and F_3 have the same features, such as misalignment angles $\alpha_1 = \alpha_3$, thickness $L_1 = L_3$, and exchange field $h_1 = h_3$. In self-consistent field method, we consider the low temperature limit and take $k_F L_{S1} = k_F L_{S2} = 400$, $\omega_D/E_F = 0.1$, the other parameters are the same as the ones mentioned above.

Fig. 2(a) shows that the critical current is a function of exchange field h_1 for the misalignment angles $\alpha_1 = \pi/2$. We find that, for the thin interface layer $k_F L_1 = 2$, the critical current I_c only has one peak at exchange field $h_1/E_F = 0.4$. With the increase of the thickness L_1 , the maximum of critical current will gradually move to the left. For the thick interface layer $k_F L_1 = 6$ and 8, the critical current I_c will display an oscillating behavior as a function of the exchange field h_1 . The oscillation frequency of critical current I_c can increase with thickness L_1 . Furthermore, for a fixed exchange field h_1 , the critical current can display the same oscillatory behavior with the change of the thickness L_1 (see fig. 2(b)). Especially, for weak exchange field $h_1/E_F = 0.2$ (blue dashed line in fig. 2(b)), the critical current I_c increases rapidly and reaches a threshold at $k_F L_1 = 3$, then slowly increases to maximum value at $k_F L_1 = 6$. Subsequently, the current will decrease at the thickness $k_F L_1 > 6$. This conclusion is well consistent with the recent work by Khaire *et al.*¹⁰ and Khasawneh *et al.*²³.

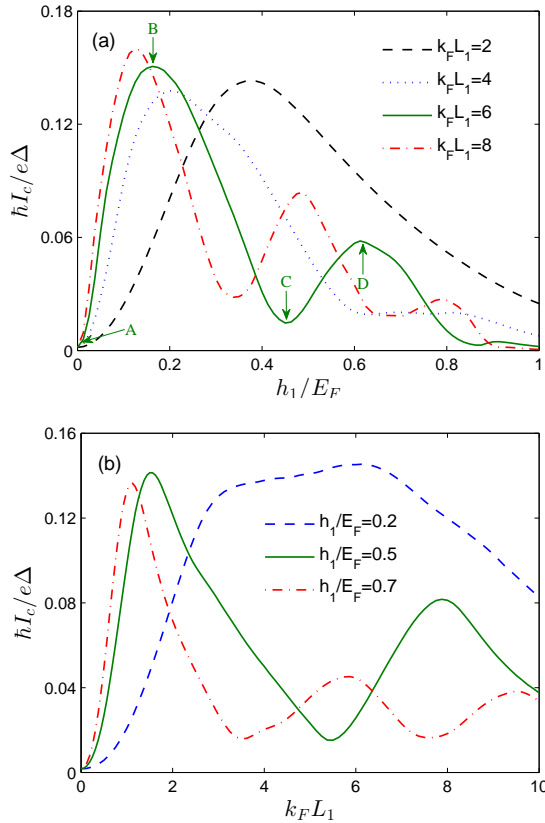


FIG. 2. (Color online) Critical current (a) as a function of the exchange field h_1 for different thicknesses L_1 and (b) as a function of the thickness L_1 for different exchange fields h_1 with $\alpha_1 = \pi/2$.

We attribute the above behavior of critical current to two important phenomena at the interface layers^{24,25}: spin mixing and spin-flip scattering process. The exchange splitting in the interface layers F_1 will lead to a modulation of the pair amplitude with $Q \cdot R$. The resulting state is mixture of spin singlet and triplet state with $S_z = 0$. When F_1 is magnetized in the same direction as F_2 (here, the z -axis), the spin singlet and triplet state projected along the z -axis, such as $(|\uparrow\downarrow\rangle - |\downarrow\uparrow\rangle)_z$ and $(|\uparrow\downarrow\rangle + |\downarrow\uparrow\rangle)_z$, can undergo damped oscillations and penetrate into F_2 a short-range. Moreover, if the interface magnetic moment in F_1 deviates from the direction of bulk magnetization in F_2 , this misalignment of the interface moment can lead to spin-flip scattering processes at the interfaces layers. The processes can be described as follows³: as shown in fig. 1, the interface layer F_1 magnetized in the x -direction will generate opposite-spin pairs with respect to the x -axis $(|\uparrow\downarrow\rangle + |\downarrow\uparrow\rangle)_x$. Such a state is equivalent to a combination of equal spin pairs. This pairs projected along the z -axis $(|\uparrow\uparrow\rangle - |\downarrow\downarrow\rangle)_z$ can propagate over a long distance into F_2 . Thus, we can get the following conclusion: long-range triplet Josephson current can modulated by $(|\uparrow\downarrow\rangle + |\downarrow\uparrow\rangle)_x$ with frequency $Q \cdot R$.

Therefore, for thin R (such as $k_F L_1 = 2$ and $k_F L_1 = 4$

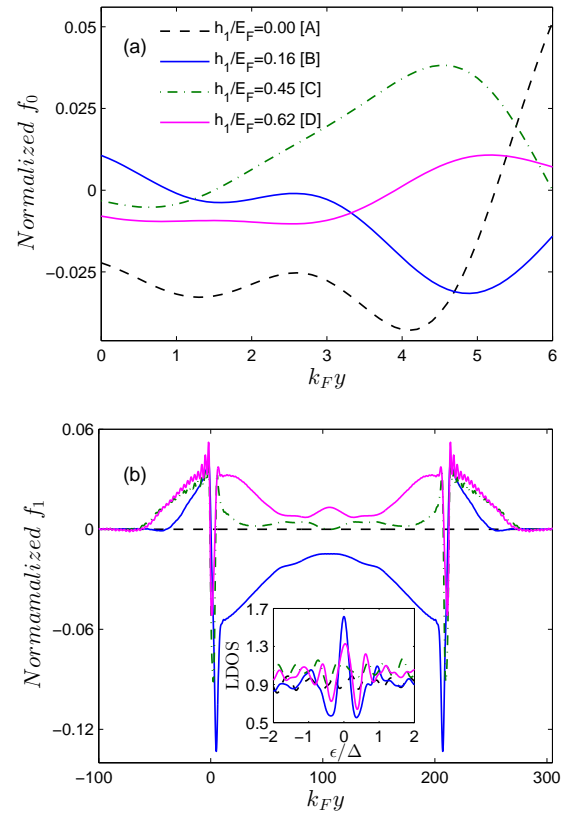


FIG. 3. (Color online) The real part of triplet pair amplitude f_0 (a) and f_1 (b) plotted as a function of the position $k_F y$ for different exchange field h_1 . Here $k_F L_1 = 6$, $\alpha_1 = \pi/2$ and $t/\omega_D = 10$. The inset in (b) is the normalized LDOS at $k_F y = 30$, which is calculate at $k_B T = 0.001$. Two panels utilize the same legend.

in fig. 2(a)), the relationship $Q \cdot R < \pi$ is always satisfied with the increase of exchange field h_1 . In this process, the spin-triplet state f_0 in F_1 will experience only one oscillation, and the critical current has only one peak. For thick R (see $k_F L_1 = 6$ and $k_F L_1 = 8$ in fig. 2(a)), $Q \cdot R$ will undergo many more $0 - \pi$ transitions, and the f_0 in F_1 has two such wobbles, or more. Then these $0 - \pi$ transitions in the phase of f_0 will lead to more peaks in the critical current. Similarly, if the h_1 is fixed and changes the L_1 , we can obtain the same conclusions (see fig. 2(b)).

To understanding the above essential physical processes, the spatial distributions of spin-triplet state are calculated in Fig. 3. The results show the real part of f_0 and f_1 for several particular exchange field $h_1 / E_F = 0, 0.16, 0.45$, and 0.62 . These exchange field correspond to the point A, B, C and D in fig. 2(a), respectively. For $h_1 / E_F = 0$, the interface layer F_1 is the normal-metal, then the spin-split and spin-flip do not exist. At this moment, the maximum of f_0 occurs close to the interface between F_1 and F_2 at site $k_F y = 6$ (black dashed line in fig. 3(a)). Then f_0 undergoes a damped oscillations in

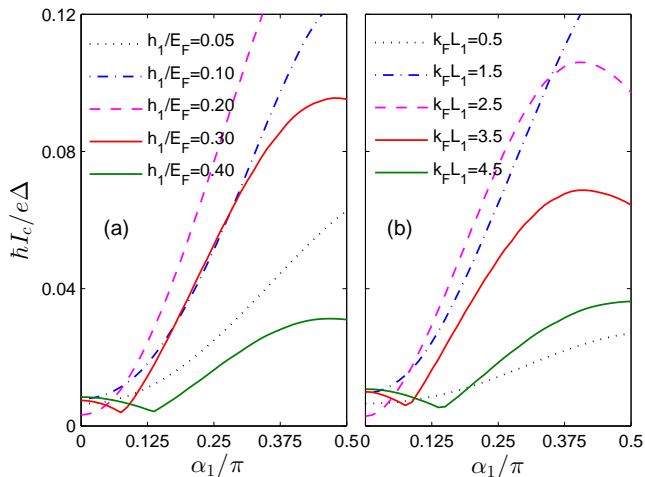


FIG. 4. (Color online) Critical current as a function of misalignment angle α_1 (a) for different exchange field h_1 when thickness $k_F L_1=6$ and (b) for different thickness L_1 when exchange field $h_1/E_F=0.5$.

F_2 , and can only penetrate a short-range. Meanwhile, f_1 doesn't survive in F_2 (black dashed line in fig. 3(b)). As a result, the critical current is almost 0. For $h_1/E_F=0.16$, f_0 oscillates in F_1 and reaches the negative maximum near the interface. In this case, f_0 projects along the x -axis due to F_1 magnetized in the x -direction. Such f_0 can be converted into the equal-spin state f_1 , which penetrates over a long distance into F_2 (see blue solid line in fig. 3(b)). Eventually, the maximal critical current can be obtained. For $h_1/E_F=0.45$, f_0 oscillates and reaches to 0 when it gets close to the interface (green dash-dotted line in fig. 3(a)). Accordingly, the amplitude of f_1 converted from the f_0 is small enough, and the critical current can be decreased. For $h_1/E_F=0.62$, f_0 returns to positive amplitude, which can produce a positive spatial distributions of f_1 . Consequently, the critical current will come back to a larger value. The above changes of the critical current can be also displayed by the LDOS, which is illustrated in the inset of fig. 3(b). For $h_1/E_F=0.16$ and 0.62 (correspond to the point B and D in fig. 2(a)), the LDOS shows a sharp zero energy conductance peak (ZCEP), which represents the long-range f_1 is large enough. When $h_1/E_F=0$ and 0.45 (correspond to the point A and C in fig. 2(a)), the ZCEP will disappear, which illustrates the f_1 doesn't exist or is very small.

In the following, we will discuss how critical current changes with the misalignment angle α_1 . We have displayed the critical current I_c change with the misalignment angle α_1 for different exchange fields h_1 when thickness $k_F L_1=6$ in fig. 4(a). For $h_1/E_F=0.05, 0.1$ and 0.2 , the current is a monotonous function of the misalignment angle α_1 . However, for $h_1/E_F=0.3$ and 0.4 , the current exhibits a nonmonotonic behavior with the increase of the misalignment angle α_1 , where the minimum occurs at some intermediate value and the maximum nearly at

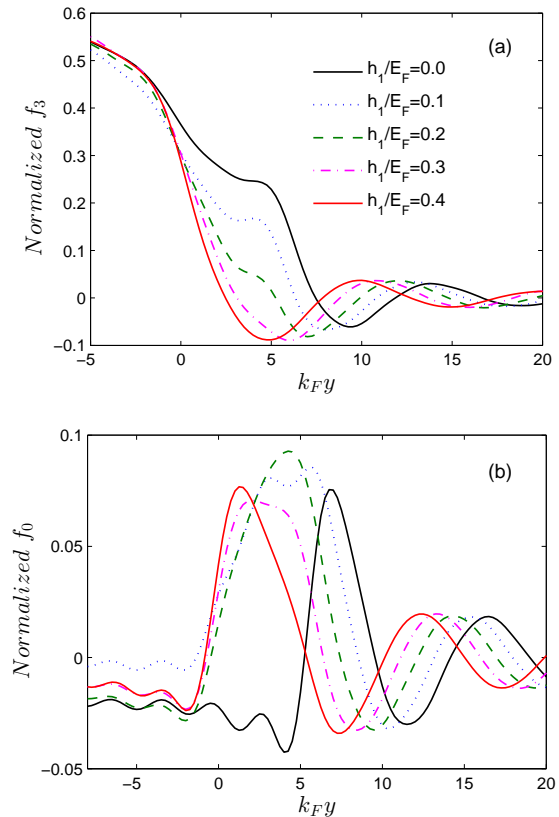


FIG. 5. (Color online) The singlet pair amplitude f_3 (a) and the real part of triplet pair amplitude f_0 (b) plotted as a function of position $k_F y$ for different h_1 . Here $k_F L_1=6$, $\alpha_1=0$, and $t/\omega_D=10$. Two panels utilize the same legend.

$\alpha_1=\pi/2$. This can be analyzed by the explanation of ref.²⁶. The above behavior of critical current is determined by the original phase of junction when the misalignment angle $\alpha_1=0$. For a particular exchange field h^* , the $0-\pi$ transition takes place in the junction just at the given thickness $k_F L_1=6$. Hence, for $h_1>h^*$ the original state of the junction with $\alpha_1=0$ is the π state, while for $h_1<h^*$ it is the 0 state. If one doesn't take absolute value for $I_e(\varphi)$ to define the critical current I_c , then I_c is all negative and monotonously decrease when α_1 changes from 0 to $\pi/2$. In this case, the original state of the junction is the 0 state. However, if the original state is π state, the I_c will decrease from a positive quantity to a negative one and reach the negative maximum nearly at the $\alpha_1=\pi/2$, then the nonmonotonic behavior mentioned beforehand would transform into monotonic, accompanying with the change of sign.

To further illustrate this behavior, we plot f_3 and the real part of f_0 at $\alpha_1=0$ and $k_F L_1=6$. In fig. 5(a), we display the spatial distributions of f_3 for four different values of exchange field h_1 . With the increase of the exchange field h_1 , the oscillations of f_3 gradually move to the left. At last, their pattern configuration in F_2 range would be reversed at $h_1/E_F\sim 0.3-0.4$. As shown in

fig. 5(b), f_0 has the same behaviors. All of these reversals predict the $0-\pi$ transition takes place with the increase of exchange field h_1 . Particularly, the above nonmonotonic behavior about the critical current I_c has been observed by Klose *et al.*¹¹ and Wang *et al.*²⁷. They apply a large magnetic field to rotate the interface magnetization. As for low fields, a shallow dip can be found in I_c . In addition, fig. 4(b) shows that the critical current I_c changes with the misalignment angles α_1 for different thickness L_1 at fixed exchange field h_1 . This behavior is same as fig. 4(a).

IV. CONCLUSION

In this article, we have calculated the Josephson current by BTK approach in clean $S/F_1/F_2/F_3/S$ junctions with noncollinear magnetization. Moreover, to demonstrate changes of the critical current, we also study the singlet and triplet pair amplitude and the local density of states in ferromagnets by using Bogoliubov's self-consistent method. We have shown that the dependence long-range triplet critical current with the strength of ex-

change field and thickness of the interface layers shows an oscillatory behavior, when the interface magnetizations are orthogonal to the central magnetization. This change of the critical current is induced by the oscillations of $(|\uparrow\downarrow\rangle+|\downarrow\uparrow\rangle)_x$ with frequency $Q \cdot R$. In addition, when the orientations of the magnetizations in interface layers rotate from z -axis to x -axis, the critical current always exhibits a nonmonotonic behavior. We have discussed the condition for this effect to be observed under the condition that the original state of the junction with the parallel magnetizations is the π state.

ACKNOWLEDGMENTS

The authors are grateful to Prof. Shi-Ping Zhou and Dr. Feng Mei for useful discussions. This work is supported by the State Key Program for Basic Research of China under Grants No. 2011CB922103 and No. 2010CB923400, and the National Natural Science Foundation of China under Grants No. 11174125 and No. 11074109.

-
- ¹ A. I. Buzdin, Rev. Mod. Phys. 77, 935 (2005).
 - ² F. S. Bergeret, A. F. Volkov, and K. B. Efetov, Rev. Mod. Phys. 77, 1321 (2005).
 - ³ M. Eschrig, Phys. Today 64, No. 1, 43 (2011).
 - ⁴ F. S. Bergeret, A. F. Volkov, and K. B. Efetov, Phys. Rev. Lett. 86, 4096 (2001);
 - ⁵ A. Kadigrobov, R. I. Shekhter, and M. Jonson, Europhys. Lett. 54, 394 (2001);
 - ⁶ Caroline Richard, Manuel Houzet, and Julia S. Meyer, Phys. Rev. Lett. 110, 217004 (2013).
 - ⁷ M. Houzet and A. I. Buzdin, Phys. Rev. B 76, 060504(R) (2007).
 - ⁸ Mohammad Alidoust and Jacob Linder, Phys. Rev. B 82, 224504 (2010).
 - ⁹ J.W. A. Robinson, J. D. S. Witt, and M. G. Blamire, Science 329, 59 (2010).
 - ¹⁰ T. S. Khaire, M. A. Khasawneh, W. P. Pratt, Jr., and N. O. Birge, Phys. Rev. Lett. 104, 137002 (2010).
 - ¹¹ Carolin Klose, Trupti S. Khaire, Yixing Wang, W. P. Pratt, Jr., and Norman O. Birge, B. J. McMorrin, T. P. Ginley, J. A. Borchers, B. J. Kirby, B. B. Maranville, and J. Unguris Phys. Rev. Lett. 108, 127002 (2012).
 - ¹² S. Hikino and S. Yunoki, Phys. Rev. Lett. 110, 237003 (2013).
 - ¹³ G. E. Blonder, M. Tinkham, and T. M. Klapwijk, Phys. Rev. B 25, 4515-4532 (1982).
 - ¹⁴ P.G. de Gennes, Superconductivity of Metals and Alloys, Benjamin, New York, 1966 (Chap.5).
 - ¹⁵ Li-Jing Jin, Yue Wang, Lin Wen, Guo-Qiao Zha, Shi-Ping Zhou, Physics Letters A 376, 2435-2441(2012).
 - ¹⁶ A. Furusaki and M. Tsukada, Solid State Commun. 78, 299 (1991).
 - ¹⁷ Z. M. Zheng and D. Y. Xing, J. Phys.: Condens. Matter 21, 385703 (2009).
 - ¹⁸ Y. Tanaka and S. Kashiwaya, Phys. Rev. B 56, 892 (1997).
 - ¹⁹ J. B. Ketterson and S. N. Song, Superconductivity, Cambridge University Press, 1999 (Part III).
 - ²⁰ Klaus Halterman, Oriol T. Valls, and Paul H. Barsic, Phys. Rev. B 77, 174511 (2008).
 - ²¹ Hao Meng, Lin Wen, Guo-Qiao Zha, and Shi-Ping Zhou, Phys. Rev. B 83, 214506 (2011).
 - ²² L. D. Landau, E.M. Lifshitz, Quantum Mechanics, Non-Relativistic Theory (third ed.) Pergamon, Elmsford, NY (1977).
 - ²³ Mazin A Khasawneh, Trupti S Khaire, Carolin Klose, William P Pratt Jr and Norman O Birge, Supercond. Sci. Technol. 24, 024005 (2011).
 - ²⁴ M. Eschrig, J. Kopu, J. C. Cuevas, and Gerd Schon, Phys. Rev. Lett. 90, 137003(2003).
 - ²⁵ M. Eschrig and T. Lofwander, Nature Phys. 4, 138 (2008).
 - ²⁶ Yu. S. Barash, I. V. Bobkova, and T. Kopp, Phys. Rev. B 66, 140503(R) (2002).
 - ²⁷ Yixing Wang, W. P. Pratt, Jr., and Norman O. Birge, Phys. Rev. B 85, 214522 (2012).